

# First-Order Type Effects in $\text{YBa}_2\text{Cu}_3\text{O}_{6+x}$ at the Onset of Superconductivity

L. Tassini, W. Prestel, A. Erb, M. Lambacher, and R. Hackl

*Walther Meissner Institut,  
Bayerische Akademie der Wissenschaften,  
85748 Garching, Germany*

(Dated: 080701)

We present results of Raman scattering experiments on tetragonal  $(\text{Y}_{1-y}\text{Ca}_y)\text{Ba}_2\text{Cu}_3\text{O}_{6+x}$  for doping levels  $p(x, y)$  between 0 and 0.07 holes/ $\text{CuO}_2$ . Below the onset of superconductivity at  $p_{\text{sc}1} \approx 0.06$ , we find evidence of a diagonal superstructure. At  $p_{\text{sc}1}$ , lattice and electron dynamics change discontinuously with the charge and spin properties being renormalized at all energy scales. The results indicate that charge ordering is intimately related to the transition at  $p_{\text{sc}1}$  and that the maximal transition temperature to superconductivity at optimal doping  $T_c^{\text{max}}$  depends on the type of ordering at  $p > p_{\text{sc}1}$ .

PACS numbers: 74.72.-h, 74.20.Mn, 78.30.-j, 78.67.-n

In cuprates the maximal transition temperature to superconductivity  $T_c^{\text{max}}$  depends on the compound class. In contrast, the variation of  $T_c$  with doping  $p$  does not, and superconductivity exists between approximately 0.05 and 0.27 holes per  $\text{CuO}_2$  formula unit in clean samples [1]. In the presence of disorder this range shrinks [1] leading to a sample-specific onset point of superconductivity at  $p_{\text{sc}1} \geq 0.05$ . In addition to superconductivity, short-range antiferromagnetism with the domains separated by quasi one-dimensional charged stripes can occur [2, 3, 4, 5, 6]. In  $\text{La}_{2-x}\text{Sr}_x\text{CuO}_4$  ( $p = x$ ), this superstructure is oriented along the diagonals of the  $\text{CuO}_2$  plane below  $p_{\text{sc}1}$  and rotates by  $45^\circ$  at  $p_{\text{sc}1}$  [7]. This rotation was also seen in the low-energy electronic Raman spectra where the ordering-related response flips symmetry [8].

For  $p > p_{\text{sc}1}$  superstructures are observed in all cuprates [3, 6, 9, 10, 11, 12]. However, the type of ordering and its relationship to superconductivity is rather complicated to pin down [5, 13, 14]. In a few compounds the lattice stabilizes static spin and charge superstructures and the superconducting transition temperature is reduced or quenched [3, 6]. In most of the cases fluctuating order prevails, and it is particularly hard to detect the charge part [5, 13]. Raman spectroscopy was found to be a viable method [8].

Inelastic (Raman) scattering of light is capable of probing most of the excitations in a solid including lattice vibrations, spins, and electrons, as well as their interactions [15]. Since the polarizations of the incident and the scattered photons can be adjusted independently, many of the excitations can be sorted out via the selection rules. For instance, the transport properties of conduction electrons can be measured independently in different regions of the Brillouin zone [15, 16], and the orientation of (fluctuating) charged stripes can be determined [8]. A detailed model calculation [17] demonstrated that in addition to the symmetry selection rules the dependence on energy and temperature of the response related to stripes can be understood quantitatively (Fig. 1) in

terms of charge-ordering fluctuations.

In this paper, we focus on the “high- $T_c$ ” compound  $\text{YBa}_2\text{Cu}_3\text{O}_{6+x}$  (Y-123) at doping levels  $0 \leq p \leq 0.07$ . The purpose is to gain insight into the nature of the onset of superconductivity at  $p_{\text{sc}1} \approx 0.06$  and into possible discrimination criteria to the “low- $T_c$ ” compound  $\text{La}_{2-x}\text{Sr}_x\text{CuO}_4$  (LSCO) studied earlier [7, 8, 17]. For  $0 < p < p_{\text{sc}1}$  we find spectral features strikingly similar to those in LSCO and conclude that the diagonal stripe-like superstructure is universal. Above  $p_{\text{sc}1}$ , the indications of the diagonal superstructure disappear. However, in clear contrast to LSCO no indications of stripe ordering are found in Y-123. Hence, the first-order type changes at  $p_{\text{sc}1}$  are not a peculiarity of LSCO [7, 8] but exist also, though with distinct differences, in Y-123. Along with that, the direct spin-spin exchange interaction and the electron-phonon coupling discontinuously de- and increase, respectively, across  $p_{\text{sc}1}$ .

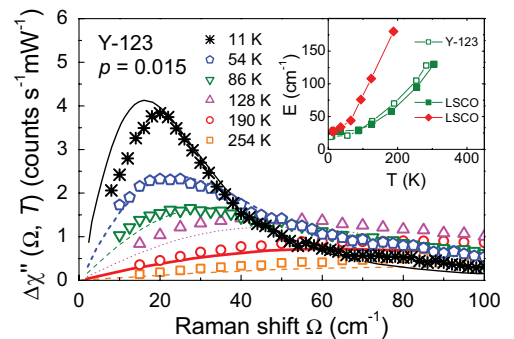


FIG. 1: (Color online) Response of charge-ordering fluctuations in  $(\text{Y}_{0.97}\text{Ca}_{0.03})\text{Ba}_2\text{Cu}_3\text{O}_{6.05}$  [17]. The points represent the experimental results, the full lines are theoretical fits. (Reproduced with permission.) Two fluctuations with finite but opposite momenta are exchanged (Azlamazov-Larkin diagrams). The inset shows the peak positions of the response as a function of temperature in  $(\text{Y}_{0.97}\text{Ca}_{0.03})\text{Ba}_2\text{Cu}_3\text{O}_{6.05}$ ,  $\text{La}_{1.98}\text{Sr}_{0.02}\text{CuO}_4$ , and  $\text{La}_{1.90}\text{Sr}_{0.10}\text{CuO}_4$ . At similar doping ( $p \approx 0.02$ ) the points essentially coincide.

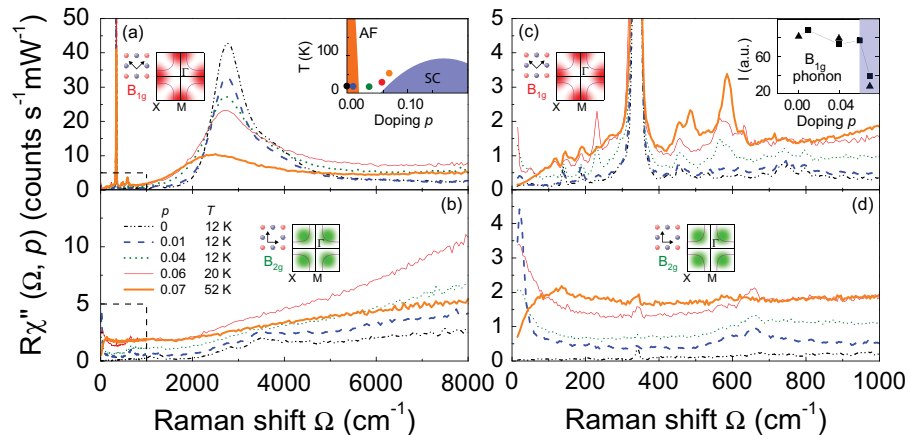


FIG. 2: (Color online) Raman response  $R\chi''(p, \Omega)$  of  $(Y_{1-y}Ca_y)Ba_2Cu_3O_{6+x}$  at low doping and temperature outside the superconducting state (raw data). The response  $R\chi''(\Omega, p)$  is obtained by dividing the experimental spectra by the Bose factor. All spectra are measured with the Ar laser line at 458 nm. The upper (a,c) and lower (b,d) panels correspond to the  $B_{1g}$  and  $B_{2g}$  symmetries, respectively, with the related polarizations and sensitivities in the Brillouin zone as indicated. Doping level and measuring temperatures of the samples are shown as full circles in the schematic phase diagram in the inset in (a), where AF and SC label antiferromagnetism and superconductivity, respectively, and are indicated explicitly in (b). Panels (a) and (b) show an energy range of  $8000 \text{ cm}^{-1}$  equivalent to 1 eV. In (c) and (d) the low-energy and intensity range is expanded as indicated by dashed boxes in (a) and (b). The inset in (c) shows the peak intensity of the  $B_{1g}$  “buckling” phonon at  $340 \text{ cm}^{-1}$  (43 meV). Triangles and squares represent Ca-free and Ca-doped Y-123, respectively.

For the studies we used single crystals of  $(Y_{1-y}Ca_y)Ba_2Cu_3O_{6+x}$  grown in  $BaZrO_3$  crucibles [18]. Doping with Ca allows us to directly control the number of holes. For  $x \simeq 0$ , doping levels up to  $p = 0.06$  are given by the Ca content,  $p = y/2$  [1]. Crystals with 0, 2, 8, and 12% Ca were studied, all not superconducting for  $x \simeq 0$ . Superconductivity could be induced only by oxygen co-doping ( $y = 0.08$ ,  $x = 0.3$ ), and  $p \simeq 0.07$  is estimated from the transition temperature  $T_c = 28 \text{ K}$  via the universal relationship  $T_c(p)$  [1]. The material remains tetragonal on the average. Hence, all samples studied here have the same crystallographic structure. We made sure that the observed effects are independent of the way of doping by also studying Ca-free crystals with  $x = 0.3$  and  $0.4$  with  $T_c = 0$  and  $26 \text{ K}$ , respectively [see Ref. [25] and inset of Fig. 2 (c)]. For  $x = 0.4$ , the superconducting sample is orthorhombic with the twin boundaries visible under polarized light. The results are identical to within the experimental uncertainty and will be published elsewhere.

In Figure 2 we show normal-state Raman spectra of Y-123 at low temperature in the doping range  $0 \leq p \leq 0.07$ . We describe first the overall trends in the energy range of  $8000 \text{ cm}^{-1}$  (1 eV).

In  $B_{1g}$  symmetry [Fig. 2 (a)] an intense phonon at  $340 \text{ cm}^{-1}$  and scattering from nearest-neighbor spin-flip excitations in the range between  $2000$  and  $4000 \text{ cm}^{-1}$  are the most prominent features observed. The evolution with doping of the magnetic scattering shows features beyond those found before [20, 21]. As long as the doping is below the onset point of superconductivity ( $p \leq p_{sc1}$ )

the peak height changes slowly and continuously while the position is essentially constant. Upon crossing  $p_{sc1}$  the two-magnon peak moves discontinuously downwards by approximately  $250 \text{ cm}^{-1}$ . Independent of doping, positions and intensities of the two-magnon peaks react only mildly when the temperature is raised [25].

In  $B_{2g}$  symmetry [Fig. 2 (b)] light scattering from spin excitations is weak [15]. A low-energy continuum appears only at finite carrier concentrations. The high-energy response increases continuously until superconductivity sets in. Then, the spectrum assumes a more convex shape and is depressed at high energy.

Zooming in on low-energies [Fig. 2 (c) and (d)] we observe a continuous increase of the electronic response upon doping in  $B_{1g}$  symmetry [Fig. 2 (c)] with no significant changes across  $p = p_{sc1}$ . On the other hand, the peak height of the  $B_{1g}$  phonon at  $340 \text{ cm}^{-1}$  collapses by factor of two for  $p > p_{sc1}$  [inset of Fig. 2 (c)].

In  $B_{2g}$  symmetry [Fig. 2 (d)] we find a complete suppression of the electronic Raman spectra below  $400 \text{ cm}^{-1}$  for  $p = 0$  as expected for an insulator. As soon as carriers are added the response becomes finite and a new peak in the range  $15$ – $30 \text{ cm}^{-1}$  pops up similar to those in  $La_{1.98}Sr_{0.02}CuO_4$  [8] and  $(Y_{0.97}Ca_{0.03})Ba_2Cu_3O_{6.05}$  (Fig. 1, [17]). Up to  $p_{sc1}$  the integrated cross section increases proportional to  $p$ . For  $p = 0.07$  it does not change any further.

In Fig. 3 we plot the low-energy  $B_{2g}$  spectra at two characteristic doping levels below and above  $p_{sc1}$  as a function of temperature in order to further highlight the qualitative changes across the critical doping. At

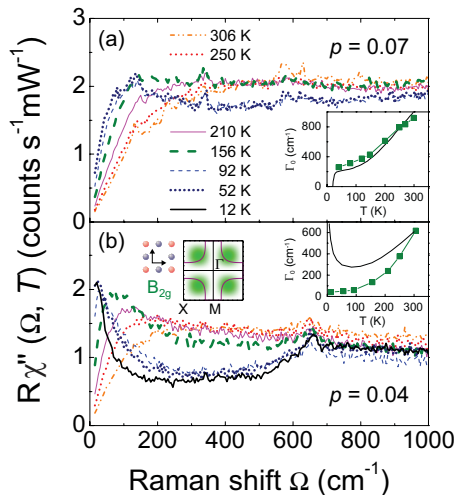


FIG. 3: (Color online) Raman response  $R\chi''_{B_{2g}}(T, \Omega)$  of  $(Y_{1-y}Ca_y)Ba_2Cu_3O_{6+x}$  at  $p = 0.07$  (a) and  $0.04$  (b). In the insets we plot the low-energy ‘‘Raman resistivities’’  $\Gamma_0(T) \propto (\partial\chi''/\partial\Omega)_{\Omega=0}^{-1}$  (squares) corresponding to the initial slope of the spectra [16] and compare them with the conventional resistivities (lines) from ref. [22].

$p = 0.07$  the response develops as expected from the resistivity and the results at  $p \geq 0.1$  [16, 22, 23] including a pseudogap of approximately  $1000 \text{ cm}^{-1}$  opening up below  $150 \text{ K}$  [16]. As shown in the inset of Fig. 3 (a) the Raman relaxation rate  $\Gamma_0(T) \propto (\partial\chi''/\partial\Omega)_{\Omega=0}^{-1}$  at low energies follows the resistivity when properly converted [16]. This is in clear contrast to the non-superconducting sample at  $p = 0.04$  where a qualitative difference between the Raman and the transport resistivities is found in the entire temperature range [inset of Fig. 3 (b)]. As can be seen in the main panel of Fig. 3 (b) the discrepancy originates from the low-energy peak developing below approximately  $250 \text{ K}$ . Along with the peak a pronounced pseudogap of approximately  $650 \text{ cm}^{-1}$  opens up which, if taken alone, could essentially account for the increase of the conventional resistivity towards low temperature. The pivotal question is as to what drives the abrupt changes versus doping level in the magnon, charge, and phonon spectra. In what follows we show that these changes are related to the superstructure in a universal way. So far, the rotation at  $p \simeq p_{sc1}$  of the essentially 1D or stripe-like pattern from diagonal to parallel with respect to the Cu–O bond direction is only established in LSCO [7], for which  $T_c^{\max} \simeq 40 \text{ K}$ . In the compounds with  $T_c^{\max}$  in the  $100 \text{ K}$  range evidence of ordering is found only at  $p \geq 0.10$ . In Y-123 [10, 11] and  $Bi_2Sr_2CaCu_2O_{8+\delta}$  [9] the order is more of checkerboard or 2D rather than of 1D or stripe type. For  $p_{sc1} < p < 0.1$ , the superstructure in Y-123 seems to disappear [24]. Very recently, nematic order was proposed to occur close to  $p \simeq 0.07$  [12]. To our knowledge, there are no experiments below  $p_{sc1}$ .

Here, we find collective modes in the Raman spectra at  $0 < p < p_{sc1}$  exhibiting shapes as well as symmetry

and temperature dependences similar to those in LSCO [8]. Apparently, they originate from the same fluctuating spin and charge superstructure with a modulation along the diagonals of the  $CuO_2$  plane (Fig. 1) [17]. We are aware that our information is not on the structure directly but only via the dynamics. However, there is no structural analysis available and the selection rules are a particularly strong argument as to symmetry breaking and orientation. In addition, shape and temperature dependence demonstrate the similarity of the underlying physics (Fig. 1). Hence, we find indications of spin and charge ordering in a completely tetragonal cuprate in the doping range between the antiferromagnet and the onset of superconductivity. The type of ordering at  $0 < p < p_{sc1}$  is universal and depends neither on the material class nor on structural details of the crystals such as lattice distortions nor on the way of doping. In fact, Ca and O doping in Y-123 lead to equivalent results [25] [for the  $B_{1g}$  phonon see inset of fig. 2 (c)]. In particular, Ca is sitting on a site with the full lattice symmetry and does not trap charges [19]. Therefore, the influence on the direction of the superstructure is expected to be weaker than that of Sr in LSCO [26] if not negligible. Alternatively, the shape of the Fermi surface can influence the orientation of the ordering in a fashion similar to nesting in materials with charge density waves [27]. With increasing doping the distance between the stripes decreases [6, 7] and the ordering wave vector  $\mathbf{q}_{\text{charge}}$  becomes large enough to connect the flat parts of the underlying Fermi surface [see, e.g., inset of Fig. 2 (c)]. Therefore, diagonal order becomes less favorable for phase space reasons and disappears above  $p_{sc1}$ . Defects may shift  $p_{sc1}$  [1].

While symmetry arguments and analogies lead to straightforward conclusions for  $p < p_{sc1}$  the analysis at  $p > p_{sc1}$  is less direct. In contrast to LSCO, where the ordering-induced collective modes change symmetry from  $B_{2g}$  to  $B_{1g}$  along with the rotation of the superstructure [8], we do not observe any ordering-related peaks in Y-123 for  $p > p_{sc1}$  [see Fig. 2 (c),  $p = 0.07$  and Ref. [8]]. However, all the renormalization effects described above demonstrate indirectly a very strong interaction peaked close to the M points, i.e. with  $|d_{x^2-y^2}|$  symmetry, [see inset of Fig. 2 (c)] to become effective at  $p > p_{sc1}$ . This interaction leads to a shift of the two-magnon peak indicating a reduction of the Heisenberg exchange coupling  $J$  by almost 10%. The related fluctuations also open a new coupling channel of proper symmetry for the  $B_{1g}$  phonon as indicated by the discontinuous reduction of the peak intensity and the onset of a (weak) Fano-type line shape. The effect on the  $\mathbf{q} \simeq 0$  Raman phonon is relatively weak in contrast to the strong coupling at  $\mathbf{q}_{\text{charge}} \simeq 0.25(2\pi/a)$  [28]. In fact, it would be interesting to study the buckling and the half-breathing phonons close to the expected  $\mathbf{q}_{\text{charge}}$  right above and below  $p_{sc1}$ .

In conclusion, superconductivity and the apparently

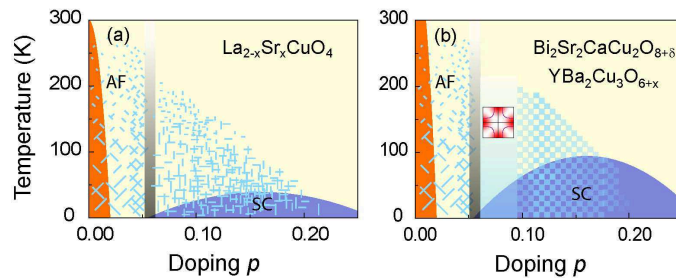


FIG. 4: (Color online) Phase diagrams for “low” (a) and “high”- $T_c$  (b) cuprates as derived from earlier [8] and present Raman data and from neutron scattering [6, 10, 11, 24] and scanning tunneling microscopy [5, 9] measurements. The position of the onset point of superconductivity  $p_{sc1}$  depends on the degree of disorder with the minimum at approximately 0.05 for clean materials [1]. The differently long lines qualitatively indicate doping and temperature ranges, density, orientation, and correlation lengths of stripes. The square pattern symbolizes checkerboard order which, however, is only established for  $p > 0.10$ . For  $p_{sc1} < p < 0.10$ , there are indications from the Raman results presented here for an interaction with structure in momentum space as sketched.

universal diagonal order at  $p < p_{sc1}$  are mutually exclusive. On the basis of the so far available results (including ours) it seems that details of the order at  $p > p_{sc1}$  are crucial for  $T_c^{max}$ . In the “low”- $T_c$  materials such as LSCO collinear stripe order prevails [2, 3, 4, 6, 7]. In compounds with  $T_c$ -s in the 100 K range the order is more 2D, e.g. of checkerboard or nematic type, aligned with the  $\text{CuO}_2$  plane [9, 10, 11, 12]. For  $p_{sc1} < p < 0.1$  we found a strongly momentum dependent interaction which is symmetry compatible with the order at  $p > 0.10$  and with the superconducting gap. Possible candidates are quasicritical fluctuations of charge stripes [29] or a fluctuating Fermi surface deformation [12, 30]. Either the electron-lattice interaction [14, 26] or details of the band structure [31] can influence the order. Combining our results with earlier ones we arrive at the phase diagrams sketched in Fig. 4.

**Acknowledgements** Discussions with T.P. Devereaux, C. Di Castro, and M. Grilli are gratefully acknowledged. The project has been supported by the DFG under grant numbers Ha2071/3 and Er342/1 via the Research Unit FOR 538 .

---

[1] J. L. Tallon, C. Bernhard, H. Shaked, R. L. Hitterman, and J. D. Jorgensen, *Phys. Rev. B* **51**, 12911 (1995).  
 [2] S.-W. Cheong, G. Aeppli, T. E. Mason, H. Mook, S. M. Hayden, P. C. Canfield, Z. Fisk, K. N. Clausen, and J. N. Martinez, *Phys. Rev. Lett.* **67**, 1791 (1991).  
 [3] J. M. Tranquada, B. J. Sternlieb, J. D. Axe, Y. Nakamura, and S. Uchida, *Nature* **375**, 561 (1995).  
 [4] A. Bianconi, N. L. Saini, A. Lanzara, M. Missori, T. Rossetti, H. Oyanagi, H. Yamaguchi, K. Oka, and T. Ito, *Phys. Rev. Lett.* **76**, 3412 (1996).  
 [5] S. A. Kivelson, I. P. Bindloss, E. Fradkin, V. Oganessian, J. M. Tranquada, A. Kapitulnik, and C. Howald, *Rev. Mod. Phys.* **75**, 1201 (2003).  
 [6] J. M. Tranquada, to appear as a chapter in “Treatise

of High Temperature Superconductivity” edited by J. Robert Schrieffer; e-print: cond-mat/0512115 (2005).  
 [7] S. Wakimoto, G. Shirane, Y. Endoh, K. Hirota, S. Ueki, K. Yamada, R. J. Birgeneau, M. A. Kastner, Y. S. Lee, P. M. Gehring, *Phys. Rev. B* **60**, R769 (1999).  
 [8] L. Tassini, F. Venturini, Q.-M. Zhang, R. Hackl, N. Kikugawa, and T. Fujita, *Phys. Rev. Lett.* **95**, 117002 (2005).  
 [9] J. E. Hoffman, K. M. Lang, V. Madhavan, H. Eisaki, S. Uchida, , and J. C. Davis, *Science* **295**, 466 (2002).  
 [10] V. Hinkov, S. Pailhes, P. Bourges, Y. Sidis, A. Ivanov, A. Kulakov, C. T. Lin, D. P. Chen, C. Bernhard, and B. Keimer, *Nature* **430**, 650 (2004), ISSN 0028-0836.  
 [11] C. Stock, W. J. L. Buyers, R. A. Cowley, P. S. Clegg, R. Coldea, C. D. Frost, R. Liang, D. Peets, D. Bonn, W. N. Hardy, *Phys. Rev. B* **71**, 024522 (2005).  
 [12] V. Hinkov, D. Haug, B. Fauqu e, P. Bourges, Y. Sidis, A. Ivanov, C. Bernhard, C. T. Lin, and B. Keimer, *Science* **319**, 597 (2008).  
 [13] C. Castellani, C. Di Castro, and M. Grilli, *J. Phys. Chem. Solids* **59**, 1694 (1998).  
 [14] H.-H. Klauss, W. Wagener, M. Hillberg, W. Kopmann, H. Walf, F. J. Litterst, M. H ucker, and B. B uchner, *Phys. Rev. Lett.* **85**, 4590 (2000).  
 [15] T. P. Devereaux and R. Hackl, *Rev. Mod. Phys.* **79**, 175 (2007).  
 [16] M. Opel, R. Nemetschek, C. Hoffmann, R. Philipp, P. F. M uller, R. Hackl, I. T utt o, A. Erb, B. Revaz, E. Walker, et al., *Phys. Rev. B* **61**, 9752 (2000).  
 [17] S. Caprara, C. Di Castro, M. Grilli, and D. Suppa, *Phys. Rev. Lett.* **95**, 117004 (2005).  
 [18] A. Erb, E. Walker, and R. Fl ukiger, *Physica C* **258**, 9 (1996).  
 [19] A. J anossy, T. Feh er, and A. Erb, *Phys. Rev. Lett.* **91**, 177001 (2003).  
 [20] S. Sugai, H. Suzuki, Y. Takayanagi, T. Hosokawa, and N. Hayamizu, *Phys. Rev. B* **68**, 184504 (2003).  
 [21] A. Gozar, S. Komiya, Y. Ando, and G. Blumberg, *Frontiers in Magnetic Materials* (Springer-Verlag, Berlin, p. 755, 2005).  
 [22] Y. Ando, S. Komiya, K. Segawa, S. Ono, and Y. Kurita, *Phys. Rev. Lett.* **93**, 267001 (2004).  
 [23] F. Venturini, M. Opel, T. P. Devereaux, J. K. Freericks, I. T utt o, B. Revaz, E. Walker, H. Berger, L. Forr o, and R. Hackl, *Phys. Rev. Lett.* **89**, 107003 (2002).

- [24] C. Stock, W. J. L. Buyers, Z. Yamani, C. L. Broholm, J.-H. Chung, Z. Tun, R. Liang, D. Bonn, W. N. Hardy, and R. J. Birgeneau, *Phys. Rev. B* **73**, 100504 (R) (2006).
- [25] L. Tassini, Doctoral Thesis, Technical University Munich (2008).
- [26] O. P. Sushkov and V. N. Kotov, *Phys. Rev. Lett.* **94**, 097005 (2005).
- [27] G. Grüner, *Density Waves in Solids* (Addison-Wesley, Reading, MA, 1994).
- [28] D. Reznik, L. Pintschovius, M. Ito, S. Iikubo, M. Sato, H. Goka, M. Fujita, K. Yamada, G. D. Gu, and J. M. Tranquada, *Nature* **440**, 1170 (2006).
- [29] A. Perali, C. Castellani, C. Di Castro, M. Grilli, E. Piegari, and A. A. Varlamov, *Phys. Rev. B* **62**, R9295 (2000).
- [30] W. Metzner, D. Rohe, and S. Andergassen, *Phys. Rev. Lett.* **91**, 066402 (2003).
- [31] G. Seibold, J. Lorenzana, and M. Grilli, *Phys. Rev. B* **75**, 100505 (R), (2007).